DNA Binding of Ruthenium Tris(1,10-phenanthroline): Evidence for the Dependence of Binding Mode on Metal Complex Concentration

Delia Z. M. Coggan,[†] Ian S. Haworth,[‡] Paula J. Bates,[§] Alan Robinson,[†] and Alison Rodger*[,†]

Department of Chemistry, University of Warwick, Coventry, CV4 7AL, U.K., Department of Pharmaceutical Sciences, University of Southern California, 1985 Zonal Avenue, Los Angeles, California 90033, and Department of Medicine, Division of Hematology/Oncology, 1824 Sixth Avenue South, University of Alabama at Birmingham, Birmingham, Alabama 35294

Received June 7, 1999

The interaction with calf thymus DNA, poly(dA-dT)$_2$ and poly(dG-dC)$_2$ of the two enantiomers (Λ and Δ) of [Ru(1,10-phenanthroline)$_3$]$^{2+}$, denoted PHEN, and of [Ru(4,7-dimethyl-1,10-phenanthroline)$_3$]$^{2+}$, denoted [4,7], [Ru(5,6-dimethyl-1,10-phenanthroline)$_3$]$^{2+}$, denoted [5,6], and [Ru(3,4,7,8-tetramethyl-1,10-phenanthroline)$_3$]$^{2+}$, denoted [3,4,7,8], has been investigated by normal absorption, linear dichroism (LD), circular dichroism (CD), and computer modeling. These studies have been performed at the saturated binding limit and the "isolated" limit where the DNA is in excess. The binding mode is dependent upon the enantiomer (Λ or Δ), the DNA base sequence, the ring substituent pattern, and, for the Δ enantiomer, the relative concentrations of DNA and metal complex. Both the Λ and Δ enantiomers of PHEN and [4,7] show at least two binding regimes. One binding regime operates below a metal complex:DNA phosphate mixing ratio, *R*, of 1:4−6. The average site size (number of DNA bases per bound metal complex) also decreases from 8−12 bases per metal complex at low *R* to 3 bases at high *R*. The average angle (α_{eff}) between the metal complex 3-fold axis and the DNA helical axis was derived from the LD. At high *R* (saturated metal complex binding) for both enantiomers of both compounds, this angle is 55° ± 3°. For low *R* (isolated metal complex binding), the average binding orientations for the enantiomers are different for PHEN (Λ, α_{eff} = 59°; Δ, α_{eff} = 38°) and for [4,7] (Λ, α_{eff} = 84°; Δ, α_{eff} = 42°). Under the low-*R* conditions the Δ enantiomer of both compounds binds to calf thymus DNA more strongly than the Λ enantiomer. [3,4,7,8] binds to DNA but is not oriented in the LD experiment. There is no evidence that [5,6] binds to DNA. To explain the LD results for PHEN several possible binding orientations were considered in computer modeling studies. These have the metal complex located with (i) a single phenanthroline chelate approximately parallel to the base pair planes in the major groove (referred to as partially inserted); (ii) a single chelate along the minor groove (referred to as slotted); (iii) two chelates in the minor groove (referred to as minor facial). Using orientations adopted in energy-minimized complexes it was possible to deduce the approximate relative occupancy of the different modes. For Λ-PHEN the partially inserted mode is favored at all mixing ratios. For Δ-PHEN at low-*R* minor groove binding is preferred for most sequences with most metal complexes adopting a minor facial orientation. However, at high *R* (close packed metal complexes) the slotted mode becomes more favorable and some major groove partial insertion also occurs. For both Δ- and Λ-[4,7] the minor facial mode is favored at low *R*. As *R* increases, the slotted mode becomes more favorable for both enantiomers of [4,7].

Introduction

[Ru(1,10-phenanthroline)$_3$]$^{2+}$ is a chiral, tris-chelate metal complex of octahedral parentage with enantiomers referred to as Λ and Δ. The helical nature of the complex, apparent in Figure 1, has previously led to speculation regarding the specificity of a given enantiomer for either right-handed or left-handed DNA duplexes.[1,2] Although the interaction of [Ru(1,10-phenanthroline)$_3$]$^{2+}$, henceforth denoted as PHEN, with DNA has been widely studied in the past decade, this apparently simple system remains only partially characterized. The early studies have been reviewed previously.[3,4] More recently, two studies in particular have made considerable progress in clarifying certain aspects of the complexation.[5,6]

There is little concensus regarding the orientation and/or the location (major groove or minor groove) of the Λ- and Δ-PHEN metal complexes in their complexes with DNA. The earliest proposal,[3] based primarily on metal complex luminescence quenching and visible absorption spectroscopy, suggested two binding modes for each enantiomer. These were both suggested to be in the major groove, with one mode having an *intercalated* phenanthroline chelate and the second mode being "surface

* Corresponding author. Phone: -44-1203-523234. Fax: -44-1203-524112. E-mail: a.rodger@warwick.ac.uk.
[†] University of Warwick.
[‡] University of Southern California.
[§] University of Alabama at Birmingham.

(1) Barton, J. K.; Basile, L. A.; Danishefsky, A.; Alexandrescu, A. *Proc. Natl. Acad. Sci. U.S.A.* **1984**, *81*, 1961−1965.
(2) Barton, J. K.; Danishefsky, A. T.; Goldberg, J. M. *J. Am. Chem. Soc.* **1984**, *106*, 2172−2176.
(3) Barton, J. K.; Goldberg, J. M.; Kumar, C. V.; Turro, N. J. *J. Am. Chem. Soc.* **1986**, *108*, 2081−2088.
(4) Haworth, I. S.; Elcock, A. H.; Freeman, J.; Rodger, A.; Richards, W. G. *J. Biomol. Struct. Dyn.* **1991**, *9*, 23−44 and references therein.
(5) Satyanarayana, S.; Dabrowiak, J. C.; Chaires, J. B. *Biochemistry* **1992**, *31*, 9319−9324.
(6) Eriksson, M.; Leijon, M.; Hiort, C.; Norden, B.; Gräslund, A. *Biochemistry* **1994**, *33*, 5031−5040.

10.1021/ic990654c CCC: $18.00
Published on Web 09/16/1999

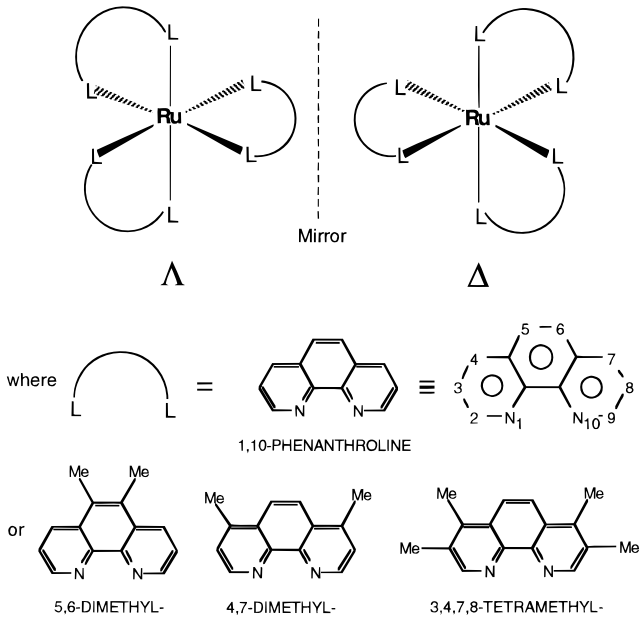

Figure 1. Structures of the two enantiomers (Λ and Δ) of [Ru(1,10-phenanthroline)$_3$]$^{2+}$, denoted PHEN, and the structure of the methyl-substituted phenanthroline chelates of [5,6], [4,7], and [3,4,7,8].

bound". In subsequent work Hiort et al.[7] concluded that each enantiomer had only one binding mode, but these differed between enantiomers, with Δ favoring a location with two chelates in the major groove and Λ having a single, *non-intercalated* chelate in the major groove parallel to the bases. These orientations were later described as *facial* and *partially inserted*, respectively.[4] The issue of intercalation vs non-intercalation was finally clarified[5] in favor of the latter, due to the relatively small change in viscosity upon PHEN complexation with DNA, compared to that for a classical intercalator. This conclusion has recently been confirmed using scanning force microscopy.[8] The luminescence data reported by Satyanarayana et al.[5] also supported a single binding mode for each enantiomer. The first suggestion of minor groove binding arose from NMR data.[9,10,11] More recent NOEs observed between metal complex and DNA protons[6] were consistent with *exclusively* minor groove binding, probably with a single chelate oriented toward the base pairs for Λ, while for Δ it was suggested that two chelates might fit in the minor groove. A number of factors may have contributed to these conflicting results. In particular, the different techniques (and hence time scales) used to probe the binding may detect certain modes more effectively than others. The different DNA sequences (and the length of duplex) used may also have some effect on the binding modes present. In addition, as we show in this paper, the binding model is a function of the metal complex:DNA concentration ratio for both enantiomers.

In this study we have characterized spectroscopically the DNA interaction of both Λ and Δ enantiomers over a greater PHEN/DNA concentration range than has previously been studied. This is the first spectroscopic investigation to consider the saturated binding limit, where the ruthenium complex is in excess and all DNA sites are occupied. The parameters that drive binding to B-DNA are probed by an investigation of equilibrium binding strengths, binding orientations, base sequence dependency, and number of binding modes, using circular dichroism (CD), linear dichroism (LD), and normal absorption (A_{iso}) spectroscopy. We have also experimentally probed the steric requirements of binding to DNA through variation of the molecular shape of the transition metal complex. This was achieved by methyl group substitution on the phenanthroline chelates giving [Ru(4,7-dimethylphenanthroline)$_3$]$^{2+}$, [Ru(5,6-dimethylphenanthroline)$_3$]$^{2+}$, and [Ru(3,4,7,8-tetramethylphenanthroline)$_3$]$^{2+}$, referred to as [4,7], [5,6], and [3,4,7,8], respectively (Figure 1).

Although CD spectra of the DNA−PHEN systems have been reported elsewhere,[7,11] only minimal attention has been paid to them. We report the changes induced into the CD spectra (ICD) of PHEN and its derivatives upon interaction with DNA. Although in principle ICD spectra could be expected to yield a great deal of geometric information,[7,12,13] in practice this is not yet possible and awaits further computational and analytic work. Qualitative and empirical analysis of the spectra are, however, very helpful for these systems since the ICD seems to be the most sensitive of all techniques to changes in binding as a function of the DNA metal complex:phosphate mixing ratio (R) (see below). For many of the systems it has been possible to determine equilibrium binding constants from ICD.

The LD spectra give a more direct measure of the relative orientation of the metal complex. Interpretation of the dichroism data is greatly aided by structural information generated from computer modeling, and, in the second part of the paper, we describe an extensive modeling study. Here we first interpret the dichroism data in terms of possible binding modes. Then, using energy minimization of metal complex/DNA complexes representative of both isolated and saturated binding conditions, we provide a semiquantitative energetic validation of the conclusions drawn from the LD results. Taken as a whole, the combined approach gives a complete description of the DNA complexation of PHEN and its methyl derivatives.

Materials and Methods

Ruthenium Compounds. $RuCl_3 \cdot 3H_2O$, (±)-Ru(1,10-phenanthroline)$_3$Cl$_2$, 4,7-dimethylphenanthroline, 5,6-dimethylphenanthroline, 3,4,7,8-tetramethylphenanthroline, potassium antimonyl *d*-tartrate, *l*-tartaric acid, and Sb_2O_3 were purchased from the Aldrich Chemical Company Ltd. The racemic ruthenium(II) tris(phenanthroline) complexes of the methylated phenanthrolines were synthesized as previously described.[14] Resolution of the Λ and Δ enantiomers from the racemic Ru(1,10-phenanthroline)$_3$Cl$_2$, as perchlorates with 95% enantiomeric purity, was performed by reaction with the antimonyl tartrate anion.[15] The differential and absolute solubilities of the diastereomers of antimonyl tartrate with the Λ and Δ enantiomers depend on the substituents of the phenanthroline chelate, making resolution by this method significantly less facile for the methyl-substituted complexes. Moderate resolution, typically 85−90% enantiomeric purity, was achieved by repeatedly adding potassium antimonyl *d*-tartrate, cooling to temperatures below 5 °C, and removing the diastereomerically impure precipitate by filtration. $NaClO_4$ was added to the final filtrate, and the Δ enantiomer was precipitated as the perchlorate. The Λ enantiomer was obtained following the same method but using potassium antimonyl *l*-tartrate. Since this was not commercially available, it was synthesized

(7) Hiort, C.; Nordén, B.; Rodger, A. *J. Am. Chem. Soc.* **1990**, *112*, 1971−1982.
(8) Coury, J. E.; Anderson, J. R.; McFailisom, L.; Williams, L. D.; Bottomley, L. A. *J. Am. Chem. Soc.* **1997**, *119*, 3792−3796.
(9) Rehmann, J. P.; Barton, J. K. *Biochemistry* **1990**, *29*, 1701−1709.
(10) Rehmann, J. P.; Barton, J. K. *Biochemistry* **1990**, *29*, 1710−1717.
(11) Nordén, B.; Patel, N.; Hiort, C.; Gräslund, A.; Seog Kyu, K. *Nucleosides Nucleotides* **1991**, *10*, 195−205.
(12) Lyng, R.; Rodger, A.; Nordén, B. *Biopolymers* **1992**, *31*, 1709−1710.
(13) Lyng, R.; Rodger, A.; Nordén, B. *Biopolymers* **1992**, *32*, 1201−1214.
(14) Lin, C. T.; Botcher, W.; Chou, M.; Creutz, C.; Sutin, N. *J. Am. Chem. Soc.* **1976**, *98*, 6536−6544.
(15) Dwyer, F. P.; Gyarfas, E. C. J. *Proc. R. Soc. N.S.W.* **1949**, *83*, 171−173.

by heating an aqueous slurry of Sb_2O_3 + KOH + *l*-tartaric acid (in molar ratio 1:1:2) under reflux for 2−3 h. As [Ru(3,4,7,8-tetramethyl-1,10-phenanthroline)$_3$]$(ClO_4)_2$ is insoluble, the tartrate salt was used in the subsequent work. Concentrations of enantiomers were determined using the extinction coefficient values[16,17] $\epsilon_{447} = 17\,000$ mol^{-1} dm^3 cm^{-1} for PHEN, $\epsilon_{442} = 19\,000$ mol^{-1} dm^3 cm^{-1} for [4,7], $\epsilon_{452} = 13\,000$ mol^{-1} dm^3 cm^{-1} for [5,6], and $\epsilon_{438} = 21\,500$ mol^{-1} dm^3 cm^{-1} for [3,4,7,8]. The differential extinction coefficient for determining enantiomeric purity was taken as $\Delta\epsilon = 6.64 \times 10^6$ mdeg mol^{-1} dm^3 cm^{-1} at 447 nm[18] for all of the metal complexes.

Polynucleotide Samples. Calf thymus DNA was purchased from Sigma, and poly(dG-dC)$_2$ and poly (dA-dT)$_2$ were purchased from Pharmacia. The DNAs, henceforth referred to as ctDNA, GC, and AT, respectively, were duplex under the experimental conditions (as shown by melting curves) and were used without further purification in 10 mM NaCl at pH = 7. Concentrations were determined spectrophotometrically using $\epsilon_{257} = 6600$ mol^{-1} dm^3 cm^{-1} for ctDNA, $\epsilon_{254} = 8400$ mol^{-1} dm^3 cm^{-1} for GC, and $\epsilon_{260} = 6600$ mol^{-1} dm^3 cm^{-1} for AT.[19,20,21]

Instruments. Normal absorption was measured on a Cary 3 spectrophotometer. CD and LD spectra were collected using a J-720 spectropolarimeter adapted for LD.

Determination of Binding Orientation. LD, at any wavelength λ, is defined as the difference in absorption of light polarized parallel and perpendicular to a macroscopic axis of orientation, in this case the flow direction in a constant shear gradient in a cylindrical Couette flow cell.[22−24] The average inclination of the 3-fold rotation axis of the metal complex with respect to the DNA helical axis, effective angle α_{eff}, can be determined from the LD spectra using the equations below,[7] which take account of perturbations caused by the electronic environment of DNA. For A_2-polarized transitions,

$$\langle \cos^2 \alpha_{eff} \rangle = \frac{1}{3} + \frac{2\,\mathrm{LD}(A_2)/S + 3\Delta A_{iso}(A_2)}{9 c_B \epsilon_F(A_2)} \qquad (1)$$

and for E-polarized transitions,

$$\langle \cos^2 \alpha_{eff} \rangle = \frac{1}{3} - \frac{2\,\mathrm{LD}(E)/S + 3\Delta A_{iso}(E)}{9 c_B \epsilon_F(E)} \qquad (2)$$

where, e.g., LD(A_2) is the LD of the A_2-polarized transition, S is the orientation parameter of the DNA, $\Delta A_{iso}(A_2)$ is the change in metal complex isotropic absorption upon mixing the metal complex with DNA, c_B is the concentration of bound metal complex, and $\epsilon_F(A_2)$ is the extinction coefficient of the A_2-polarized transition of the free metal complex. If the E degeneracy is lifted upon DNA binding, then, to a first approximation (particularly if the ruthenium coordination sphere is not significantly geometrically distorted), eq 2 is still appropriate as the near degenerate formerly E components will still occur at approximately the same wavelengths and the unperturbed component absorptions are degenerate and therefore of equal magnitude.

For PHEN and its methylated derivatives the spectroscopy of the isolated molecule is probably the greatest hindrance to interpretation of LD data since it is so complicated.[25−27] The metal complex has D_3 symmetry, so the 4d orbitals split to occupied e(d), a_1(d), and unoccupied e(d) energy levels. The chelate π and π^* orbitals are either symmetric (a_1 + e) or antisymmetric (a_2 + e) with respect to the C_2 axes (Figure 1) of the molecule. The d and chelate orbitals are very close in energy, and the extent of their interaction is unclear.

For our purposes we need a clear assignment (A_2 or E) at one point in the spectrum. It is generally agreed that the polarization is pure at ∼485 nm; however, there is debate as to what the polarization should be. Previously[7] we assigned the transition at 480 nm to be an A_2-polarized charge transfer transition. This assignment followed from consideration of the CD spectrum of the free transition metal complex.[28] However, more recent flourescence anisotropy measurements on a range of related compounds performed by Lincoln and Nordén lead to the conclusion that this region of the specrum is E polarized and in fact the degeneracy is lifted upon DNA binding. For many of the PHEN orientations determined below from LD, the assignment does not matter, as the angles are ∼55°. However, for some cases it is important. We have followed the assignment of Lincoln and Nordén, and indeed confirmed their assignment because of the correlation between % occupancy of binding sites and the binding energies in those sites.

A_{iso} and LD experiments were run in parallel for the ctDNA complexes of PHEN, [4,7], [3,4,7,8], and [5,6] over the wavelength region 300−600 nm. The absorption in the wavelength region >300 nm is dominated by the (perturbed) transitions of the metal complex. Since the isolated metal complex is not oriented by the flow apparatus, nonzero LD in this region is a direct visualization of those metal complexes associated with, and oriented by, the DNA.

The LD spectra were recorded as a titration series in 10 mM NaCl. The metal complex concentration was kept constant in any one series (the exact concentrations are shown in the figures). The DNA concentration was increased from 0 μM by adding small aliquots of a stock solution containing the required metal complex concentration, 10 mM NaCl, and approximately 3500 μM DNA phosphate. The induced A_{iso} (ΔA_{iso}) spectra were obtained by subtracting the intrinsic normal absorption of the unbound metal complex (at the appropriate concentration) from the normal absorption of samples prepared as for the LD.

Determination of the Orientation Factor, *S*. The LD signal of oriented pure ctDNA between 230 and 300 nm results from transitions of the purine and pyrimidine bases. Because these planar base pairs are essentially perpendicular to the helix axis, and this is the axis of orientation, the base $\alpha_{eff} \sim 90°$. Hence S can be found from the LD of DNA in the 260 nm band.[7] S is reduced upon addition of Δ-PHEN by about a factor of 2.[7] However, in the results given below, α_{eff} is close to the magic angle at the low DNA phosphate:metal complex ratios where this is a problem, so an error of only about 1° is introduced by ignoring the orientation reduction.

Equilibrium Binding Constants from CD. The CD experimental details for both enantiomers of PHEN, [4,7], [5,6], and [3,4,7,8] with ctDNA are the same as those outlined above for the LD titrations. The DNA complexes of PHEN and [4,7] were further probed using the synthetic DNA duplexes, AT and GC. For these spectra, the titrations involved a starting solution containing 60 μM metal complex and either AT or GC of approximate concentration 750 μM in 10 mM NaCl. The metal complex:DNA phosphate ratio (R) was gradually increased by addition of 60 μM metal complex in 10 mM NaCl. Thus for all titrations the metal complex concentration remained constant while the DNA concentration was systematically either increased or decreased. This facilitates comparison between different R as the change in ICD (or LD or ΔA_{iso}) is due to changes in the ratio of bound to free metal complex and changes in binding, but not to changes in the total metal complex concentration. The induced CD (ICD) spectra were obtained by subtracting the intrinsic CD of the free ruthenium metal complexes at the appropriate concentrations.

Analysis of the ICD spectra as a function of R may indicate the number of binding modes/regimes. When either a single binding mode or single binding regime (more than one site occupied but with constant

(16) Mesmaeker, A. K.-D.; Nasielski-Hinkens, R.; Maetens, D.; Pauwels, D.; Nasielski, J. *Inorg. Chem.* **1984**, *23*, 377−379.
(17) Bonati, F.; Cenini, S.; Morelli, D.; Ugo, R. *J. Chem. Soc. A* **1966**, 1050−1052.
(18) Eriksson, M.; Leijon, M.; Hiort, C.; Nordén, B. *J. Am. Chem. Soc.* **1992**, *114*, 4933−4934.
(19) Wells, R. D.; Larson, J. E.; Grant, R. C.; Shortle, B. E.; Cantor, C. E. *J. Mol. Biol.* **1970**, *54*, 465−497.
(20) Inman, R. B.; Baldwin, R. L. *J. Mol. Biol.* **1962**, *5*, 172−184.
(21) Felsenfeld, G.; Hirschman, S. Z. *J. Mol. Biol.* **1965**, *13*, 409−419.
(22) Michl, J.; Thulstrup, E. W. *Spectroscopy with Polarized Light*; VCH Publishers Inc.: New York, 1986.
(23) Nordén, B.; Kuruscev, T. *Q. Rev. Biophys.* **1992**, *25*, 51−170.
(24) Rodger, A. In *Metallobiochemistry, Part C: Spectroscopic and Physical Methods for determination of Metal Ion Environments in Metalloenzymes and Metalloproteins*; Riordan, J. F., Vallee, B. L., Eds.; Vol. 226, pp 232−258.
(25) Belser, P.; Daul, C.; Zelewsky, A. *Chem. Phys. Lett.* **1979**, 596.
(26) Crosby, G. A.; Hipps, K. W. *J. Am. Chem. Soc.* **1975**, *97*, 1211.
(27) Lyte, F. E.; Hercules, P. M. *J. Am. Chem. Soc.* **1969**, *91*, 253.
(28) Schipper, P. E.; Rodger, A. *J. Am. Chem. Soc.* **1983**, *105*, 4541−4550.

relative proportions) is occupied, the metal complex ICD is proportional to the concentration of bound metal complex, c_B, so $c_B = \xi\rho$, where ξ is a proportionality constant and ρ is the ICD signal at a given wavelength.[24,29,30] So, if qualitative inspection of the ICD spectra across a titration series reveals a change in *spectral form*, then this is a positive indication of a concentration dependent change of binding regime. This may be either a change in the relative proportion of binding modes present and/or the emergence of a new binding mode.

Submatrix analysis[16] is a sensitive factor analysis technique which may be used to assess the number of significant components (modes or regimes) contributing to the ICD spectral changes over the course of a DNA−metal complex titration series. Factor analysis will decompose a submatrix of the total titration data matrix constructed from the spectra of the m lowest R to give m eigenvalues (λ_j). If this procedure is conducted for all submatrices of the data matrix (from $m = 2$ to $m =$ [the total number of spectra in titration series]), a plot of the natural logarithm of each normalized eigenvalue at the position on the abscissa corresponding to m (the number of spectra) shows changes in binding across that series graphically. Eigenvalues associated with noise or species at relatively low concentrations are small and cluster at natural logarithm values below −6, whereas eigenvalues derived from absorbing species at relatively high concentrations are large and lie toward 0.

Empirical analysis of the ICD spectra in a constant binding regime using the intrinsic method (IM)[24,30] can establish the effective binding site size (by which we mean the number of bases per bound metal complex) and is the simplest measure of the binding strength (the equilibrium binding constant), as long as the binding is noncooperative.[31,32] The method fails if the binding is cooperative or if there is no uniform binding regime, so it only gives an answer for situations where it is valid. As the IM does not require measurements for a limiting case where all metal complexes are bound, this method is ideally suited to systems where different binding behavior is operative in different concentration regions.

Computer Modeling. To investigate differences between the "isolated" metal complex binding and "saturated" metal complex binding (referred to above as low-*R* and high-*R* binding, respectively), several different complexes were used. These were, using the AT-alternating heteropolymer as an example, (i) a decamer duplex, for example, $(dAdT)_5$·$(dAdT)_5$ with a single metal complex positioned at the central (5′-ApT) base pair step; (ii) a 14-mer duplex $(dAdT)_7$·$(dAdT)_7$, again with a metal complex positioned at the central step, but also with two flanking metal complexes at the 5′-ApT steps neighboring the central step; and (iii) an 18-mer duplex $(dAdT)_9$·$(dAdT)_9$, with five metal complexes positioned at the central five 5′-ApT steps. Similar sets of calculations were performed with $(dGdC)_n$·$(dGdC)_n$, $(dCdG)_n$·$(dCdG)_n$, $(dTdA)_n$·$(dTdA)_n$, $(dGdT)_n$·$(dAdC)_n$, $(dA)_n$·$(dT)_n$, $(dG)_n$·$(dC)_n$, and several other mixed sequences, although not exhaustively in each case. In the $(dCdG)_n$·$(dCdG)_n$ and $(dTdA)_n$·$(dTdA)_n$ helices the metal complexes are constrained to occupy 5′-py-p-pu sites, which we have previously shown to be unfavorable toward PHEN binding[33] compared with 5′-pu-p-py sites.

Three different metal complex orientations were used. Briefly, the three binding modes are referred to as *partially inserted* (one chelate in the major groove), *slotted* (one chelate in the minor groove), and *minor facial* (two chelates in the minor groove). For a given multimetal complex/DNA complex calculation, each metal complex had the same orientation. Complexes were constructed using canonical B-DNA built with the QUANTA4.0 package. The metal complex geometries were based on the crystal structure of [Ru(4,7-diphenylphenanthroline)$_3$]$^{2+}$.[34] Maximum symmetry was initially maintained in constructing the complexes. Subsequently, starting points that deviated from high symmetry were created to ensure that global energy minima were located. To increase the reliability of comparison between Λ and Δ complexes, similarly oriented binding modes were obtained by overlaying the "unique chelate" (in the slotted and inserted complexes the chelate pointing into the groove and in the facial complexes the chelate pointing out of the groove) in the two enantiomers. With the minor facial binding mode it is difficult to decide what the most appropriate starting metal complex orientation should be, since rotation about an axis coaxial with the pseudo-2-fold axis of the DNA produces an infinite number of, at first sight, equally valid orientations. To assess minor groove facial binding for PHEN we therefore built a series of single metal complex minor groove facial complexes for Λ and Δ, with each complex having a different angle between the plane of the single chelate oriented away from the groove and the plane of the base pairs.

Energy minimizations were performed for each complex using the AMBER4.0.1 force field.[35,36] In these calculations the PHEN metal complex was flexible, but the dihedral angle (θ) that defines the spatial orientation of the metal complexes with respect to the 3-fold axis of the complex was constrained to its value in the crystal structure of [Ru(4,7-diphenylphenanthroline)$_3$]$^{2+}$. In applying this constraint, θ was defined for each chelate from one N atom of the chelate through two dummy atoms on the metal complex 3-fold axis to the second N atom of the same chelate. Several other bond length and bond angle restraints were also applied to retain the crystal geometry around the ruthenium atom. Other force field parameters and point charges used to describe the metal complexes have been described previously.[4] Standard AMBER parameters were applied to the DNA. Following a brief minimization of the metal complex(es) only, each metal complex/DNA complex was subjected to a total of 6000 steps of conjugate gradient energy minimization using a nonbonded cutoff of 12 Å and a distance-dependent dielectric ($\epsilon = 4r_{ij}$). In the first 3000 steps, force constants of 50 kcal/mol/Å were applied to all of the internal geometrical constraints set on the metal complex. In the next 2000 steps these force constants were reduced to 25 kcal/mol/Å, and subsequently to 10 kcal/mol/Å for the final 1000 steps.

The binding energies of the single metal complex complexes were calculated as a sum of the deformation energy of the DNA (relative to a minimized free DNA duplex) caused by metal complex binding and the metal complex/DNA interaction energy. In the multiple metal complex complexes we calculated a binding energy for each metal complex using a DNA deformation energy equal to 1/n of the total deformation (where n is the number of metal complexes). In all of the energy analyses we omitted the terminal base pairs.

To facilitate comparison with the LD spectra, we also extracted the angle between the metal complex 3-fold axis (for the multimetal complex calculations, that for the central metal complex) and the DNA helical axis. To obtain the vector of this latter axis we analyzed each minimized duplex using the CURVES3.1 algorithm.[37,38] The vector of the metal complex 3-fold axis was computed and visualized with a program VECANG97 written specifically for this purpose. VECANG97 also determines the angle between the metal complex 3-fold axis and the CURVES3.1 generated DNA helical axis.[39]

Results and Discussion

ΔA_{iso} Spectra. The ΔA_{iso} spectra shown for PHEN, [4,7], and [3,4,7,8] in Figures 2 and 3 are the differences between the absorbance of the metal complexes in the presence and absence of ctDNA. The profiles of the visible absorption band for both [5,6] enantiomers are unchanged on addition of DNA (data not

(29) Rodger, A.; Blagborough, I. S.; Adlam, G.; Carpenter, M. L. *Biopolymers* **1994**, *34*, 1583−1593.
(30) Rodger, A.; Nordén, B. *Circular dichroism and Linear Dichroism*; Oxford University Press: Oxford, 1997.
(31) McGhee, J. D.; von Hippel, P. H. *J. Mol. Biol.* **1974**, *86*, 469−489.
(32) McGhee, J. D.; von Hippel, P. H. *J. Mol. Biol.* **1976**, *103*, 679.
(33) Haworth, I. S.; Elcock, A. H.; Rodger, A.; Richards, W. G. *J. Biomol. Struct. Dyn.* **1991**, *9*, 553−569.
(34) Goldstein, B. M.; Barton, J. K.; Berman, H. M. *Inorg. Chem.* **1986**, *25*, 842−847.
(35) Pearlman, D. A.; Case, D. A.; Caldwell, J. C.; Seibel, G. L.; Singh, U. C.; Weiner, P.; Kollman, P. A. *AMBER4.0*; University of California: San Francisco, 1991.
(36) Weiner, S. J.; Kollman, P. A.; Nguyen, D. T.; Case, D. A. *J. Comput. Chem.* **1986**, *7*, 230−252 and references therein.
(37) Lavery, R.; Sklenar, H. *J. Biomol. Struct. Dyn.* **1988**, *6*, 63−91.
(38) Ravishanker, G.; Swaminathan, S.; Beveridge, D. L.; Lavery, R.; Sklenar, H. *J. Biomol. Struct. Dyn.* **1989**, *6*, 669−699.
(39) Haworth, I. S.; Rodger, A. Unpublished results.

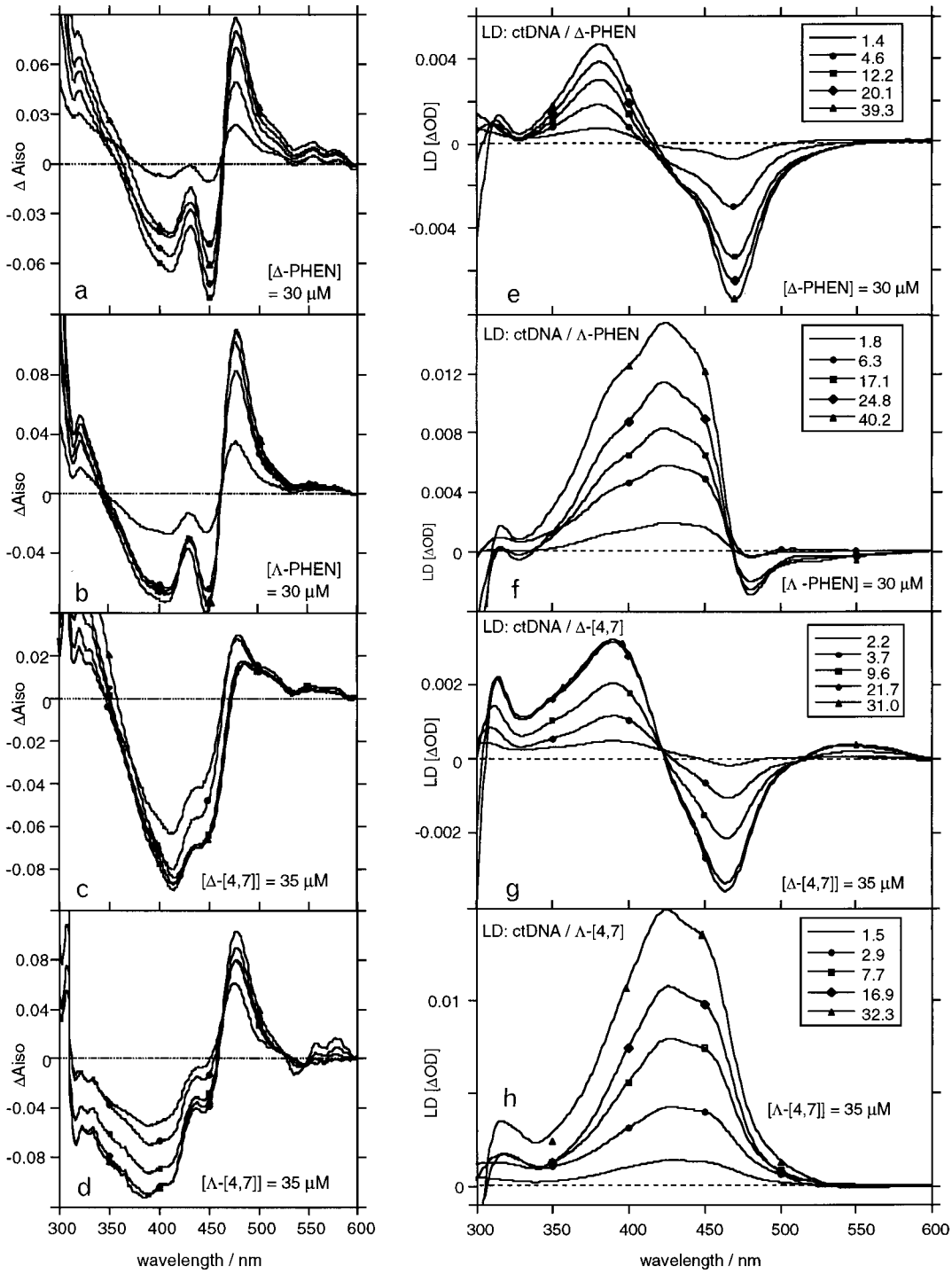

Figure 2. ΔA_{iso} spectra for ctDNA with (a) Δ-PHEN, (b) Λ-PHEN, (c) Δ-[4,7], and (d) Λ-[4,7] LD spectra for ctDNA with (e) Δ-PHEN, (f) Λ-PHEN, (g) Δ-[4,7], and (h) Λ-[4,7]. Metal complex concentrations are given in each figure. Spectra (and hence DNA concentrations) are labeled by the 1/*R* values on the LD spectra. All spectra were run in 10 mM NaCl, pH = 7 with 18.2 MΩ water.

shown). ΔA_{iso} could be used as input to the IM, but the ICD is more sensitive to binding, so our analysis of ΔA_{iso} is purely qualitative.

The visible absorption bands of the DNA complexes of PHEN, [4,7], and [3,4,7,8] are slightly hypochromic and blue-shifted relative to the free metal complex spectra for both the Δ and Λ enantiomers (Figure 2). Both Λ-[4,7] and Λ-[3,4,7,8] have significantly larger ΔA_{iso} positive maximum:negative maximum ratios than those for the corresponding Δ enantiomers. The Λ-PHEN vs Δ-PHEN difference is less distinct. The intensity around 450 nm decreases by approximately 15% for the 1:30 ratio spectra. Isosbestic points occur in the ΔA_{iso} spectra as follows: Δ-PHEN, 468 nm; Λ-PHEN, 463 nm; Δ-[4,7], ~470 nm; Λ-[4,7], 467 nm; Δ-[3,4,7,8], 452 nm; Λ-[3,4,7,8], 448 nm. The ΔA_{iso} spectra are consequently all positive in the 485 nm region of the metal to metal complex charge transfer (MLCT) band and negative in the 400 nm region. The assignment of the 400 nm region of this band to an A_2-polarized transition follows the analysis of the LD spectrum for the Δ complexes (see below). It may or may not be the A_2 component of the first MLCT band. Our initial assumption had been that the first MLCT A_2 component occurred at about 450 nm. However, analysis of the E LD (see below) indicated an angle of 30−40° between the metal complex 3-fold axis and the DNA

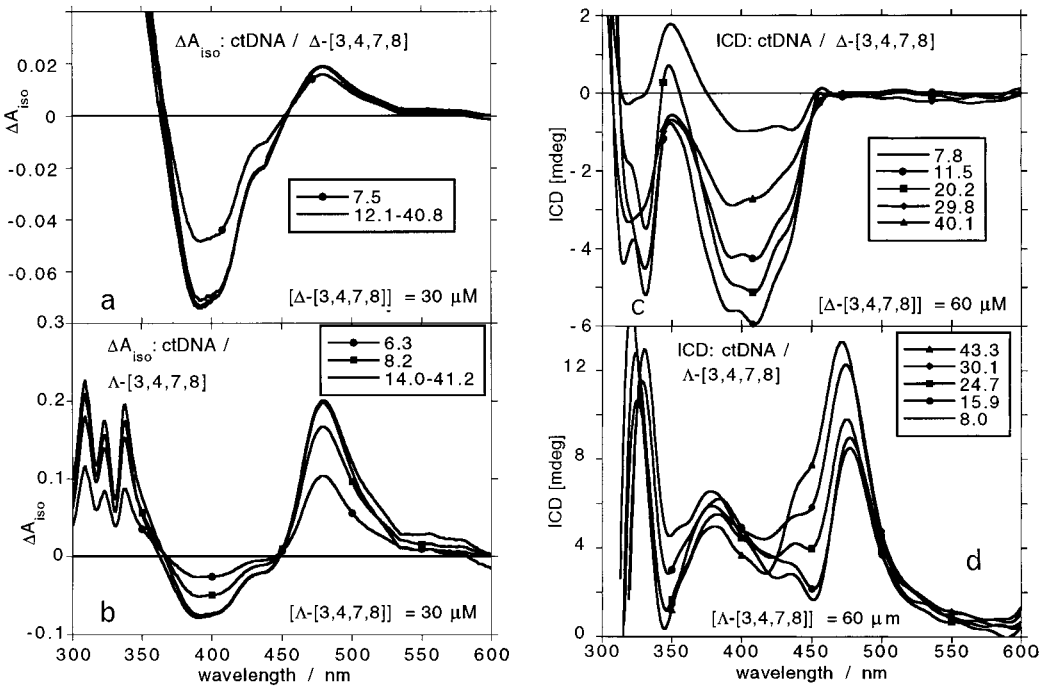

Figure 3. ΔA_{iso} spectra for ctDNA with (a) Δ-[3,4,7,8] and (b) Λ-[3,4,7,8] and LD spectra for ctDNA with (c) Δ-[3,4,7,8] and (d) Λ-[3,4,7,8]. Metal complex concentrations are given in each figure. Spectra (and hence DNA concentrations) are labeled by the 1/*R* values on the LD spectra. All spectra were run in 10 mM NaCl, pH = 7 with 18.2 MΩ water.

helix axis. In the absence of a perturbative contribution to the LD,[7] the A_2 LD should therefore be positive. This still holds when the perturbation is included since the large orientation contribution to the LD will dominate the perturbation LD of Δ (this is not necessarily true for the smaller Λ LD). Thus if the 500 nm absorbance is E polarized, the minimum at 450 nm cannot be dominated by an A_2-polarized transition (see below for further discussion).

LD Spectra. The LD for PHEN and [4,7] with ctDNA are illustrated in Figure 2. When bound to DNA, the Δ-PHEN enantiomer displays two LD bands of opposite sign in the visible region. The negative band with a maximum at 470 nm and a shoulder at 430 nm has a slightly larger magnitude relative to the positive band (maximum at 380 nm). There is no obvious change in LD spectral form across a titration series of *R* 1:1 to 1:35. In contrast to previous work,[7] although all spectra have zero signal near 420 nm, there is no clear isosbestic point. The LD spectra of the Δ-[4,7] enantiomer have a very similar form to those of PHEN. This indicates that the binding orientation is virtually unaffected by the methyl groups in the 4 and 7 positions.

When oriented by DNA at *R* less than 1:4, Λ-PHEN displays one strong, structured positive LD band at 425 nm with a shoulder at 385 nm and a very small negative indication at 480 nm. There is an approximate isosbestic point at 470 nm at smaller *R*. The bound Λ-[4,7] enantiomer has no negative signal over all *R* and a positive LD band at 425 nm across the range of *R* 1:1 to 1:35. At high binding ratios there is little difference between Λ-PHEN and Λ-[4,7], but as binding ratio decreases, the spectra become less similar.

There is no detectable LD signal for Δ-[3,4,7,8], Λ-[3,4,7,8], Δ-[5,6], or Λ-[5,6] with ctDNA (data not shown). However, as both enantiomers of [3,4,7,8] give rise to ΔA_{iso} and ICD signals, specific and hence oriented binding is indicated. The DNA LD signal in the 300−200 nm region is reduced in the presence of both Δ-[3,4,7,8] and Λ-[3,4,7,8], suggesting that the metal complexes prevent DNA from orienting in the flow field. By way of contrast, the [5,6] metal complexes have virtually no ΔA_{iso} or ICD signal and the DNA LD remained unchanged as the metal complex concentration increased, so the lack of a metal complex LD signal is direct evidence for no oriented binding to the DNA helix.

Table 1. Average Orientation, α_{eff}, of the Metal Complex 3-Fold Axis with Respect to the ctDNA Helix Axis as Determined from the 485 nm LD and ΔA_{iso} Spectra (Figure 2) Assuming That the Transitions Are E Polarized at 485 nm as Discussed in the Text[a]

		E-polarized transition at 485 nm		
metal complex	*R*	$\Delta A_{iso}/A_{iso}$	LD	α_{eff}, deg
Δ-PHEN	1:24	0.561	−0.0040	38 ± 2
	1:1.8	0.258	−0.0010	53 ± 4
Λ-PHEN	1:20	0.771	−0.0016	59 ± 4
	1:2.8	0.234	−0.0003	57 ± 4
Δ-[4,7]	1:23.8	0.075	−0.0022	42 ± 3
	1:1.9	0.120	−0.0004	54 ± 4
Λ-[4,7]	1:22	0.396	0.0023	84 ± 6
	1:2	0.294	0.0004	58 ± 4

[a] *R* is the mixing ratio metal complex:DNA phosphate.

Under the conditions of the flow experiments, an average value of $S = 0.0057$ (cf. eqs 1 and 2) was determined from the reduced LD of ctDNA at 250 nm in the middle of the first DNA absorption band. The limitations of this procedure were discussed above. The α_{eff} for PHEN and [4,7] were determined using eq 2[7] from the LD and ΔA_{iso} values at 485 nm assuming it is dominated by an E-polarized transition. The results are summarized in Table 1. At low *R* the angles presented in this study are thus not entirely consistent with previous work[7,40] since this transition was previously assumed to be A_2 polarized as discussed above. The binding orientations have not been previously reported at high drug load (i.e., at high *R*). The indicated α_{eff} error range takes account of the difference between titrations within the mixing ratio range studied.

ICD Spectra. The ICD spectra of DNA complexes of Δ-PHEN and Λ-PHEN are shown in Figure 4, and those of

(40) Yamagishi, A. *J. Chem. Soc., Chem. Commun.* **1983**, 572−573.

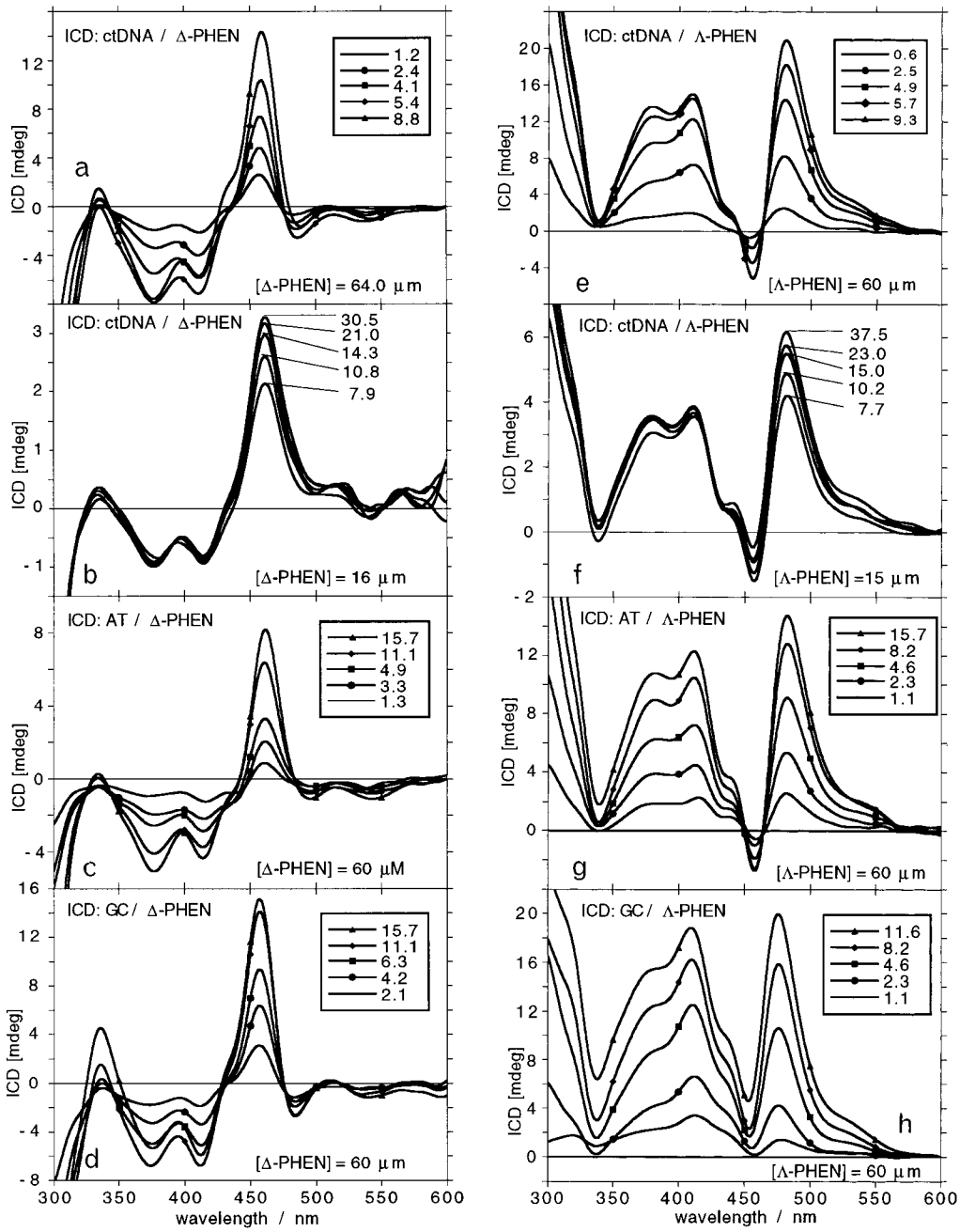

Figure 4. ICD spectra for Δ-PHEN with (a) ctDNA at high metal complex concentration, (b) ctDNA at low metal complex concentration, (c) AT DNA, and (d) GC DNA and ICD spectra for Λ-PHEN with (e) ctDNA at high metal complex concentration, (f) ctDNA at low metal complex concentration, (g) AT DNA, and (h) GC DNA. Metal complex concentrations are given in each figure. Spectra (and hence DNA concentrations) are labeled by the 1/*R* values on the LD spectra. All spectra were run in 10 mM NaCl, pH = 7 with 18.2 MΩ water.

Δ-[4,7] and Λ-[4,7] are shown in Figure 5. Changes in the form of the ICD spectra, indicative of multiple binding modes, are observed with both enantiomers of PHEN and of [4,7]. The shape of the ICD spectra of the Δ-PHEN and Λ-PHEN complexes changes at a mixing ratio in the region 1:4−6 and is more pronounced in the case of the Δ enantiomer. The Δ-[4,7] complex displays a change in spectral form at a similar mixing ratio, but the change for the Λ-[4,7] system occurs at a lower ratio (*R* equals 1:2−4) and is distinctive. These observations are supported by submatrix analysis (data not shown): second and third eigenvalues become evident, relative to the noise values, in the respective *R* regions. As there is no evidence of excitonic Ru−Ru interactions, this suggests that there is more than one binding mode and, at higher DNA concentrations, less favorable sites or modes are vacated.

For a given metal complex, the variation in spectral form with differing polynucleotides is generally small. ICD spectra of Λ-PHEN and Λ-[4,7] with AT and GC differ slightly, the difference being greater at high *R*. In the Λ-[4,7]−DNA systems, the distinctive changeover in spectral form across the titration series occurs at slightly lower *R* for AT (1:3−4) than for GC (1:2−3). The mixed base composition of ctDNA is reflected by the shape of the ICD signal, which may be approximately constructed by combining the corresponding AT and GC spectra.

The ICD spectra of the DNA−[3,4,7,8] systems are shown in Figure 3. At *R* greater than 1:15, both the Δ-[3,4,7,8] and Λ-[3,4,7,8] caused aggregation of ctDNA, resulting in fluctuations in the relative and actual concentrations of the DNA and ruthenium complexes in solution. In the region of mixing ratios 1:8 to 1:30 a change in ICD spectral form occurs which is more

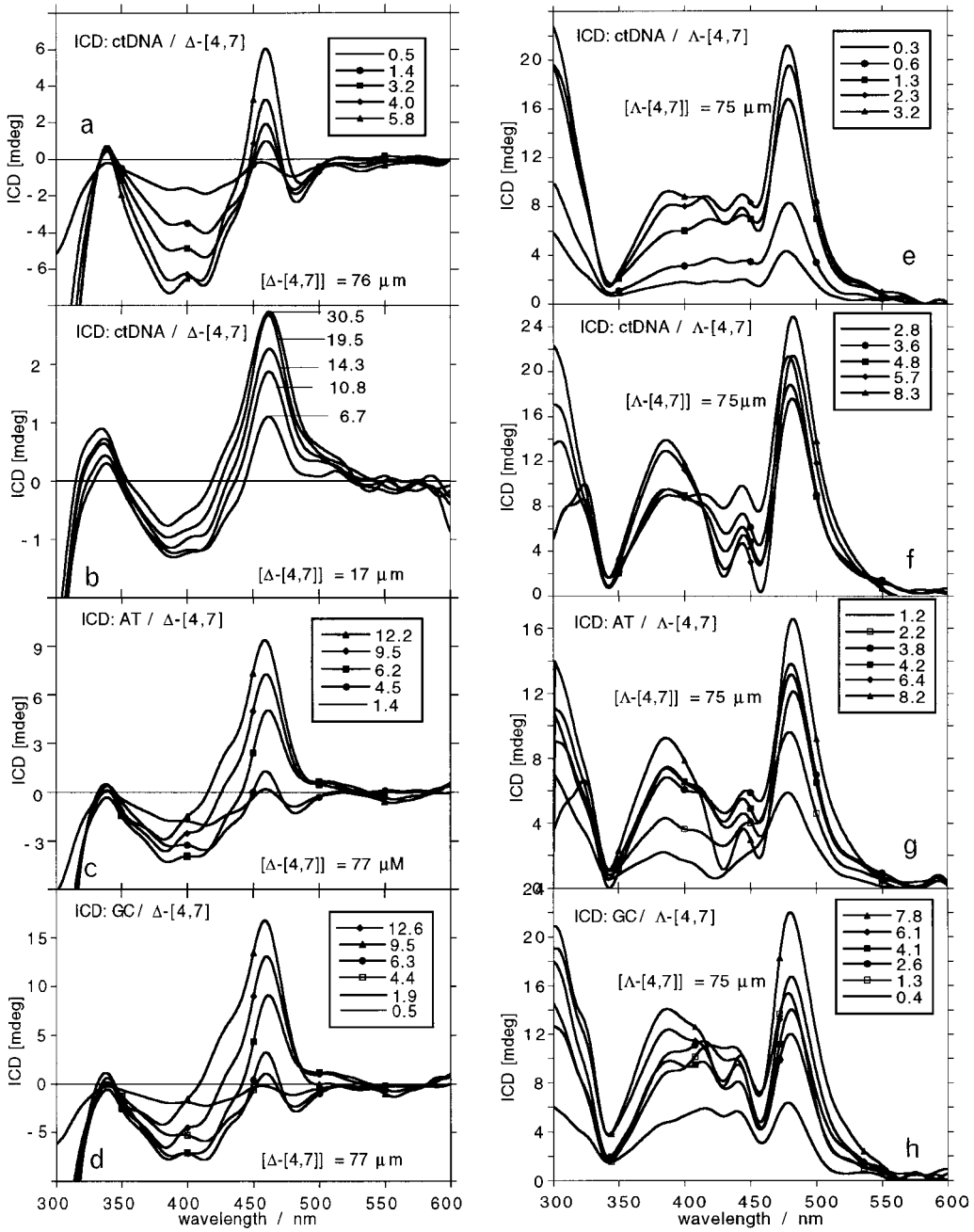

Figure 5. ICD spectra for Δ-[4,7] with (a) ctDNA at high metal complex concentration, (b) ctDNA at low metal complex concentration, (c) AT DNA, and (d) GC DNA and ICD spectra for Λ-[4,7] with (e) ctDNA at high metal complex concentration, (f) ctDNA at low metal complex concentration, (g) AT DNA, and (h) GC DNA. Spectra (and hence DNA concentrations) are labeled by the 1/*R* values on the LD spectra. All spectra were run in 10 mM NaCl, pH = 7 with 18.2 MΩ water.

pronounced for Λ-[3,4,7,8]−ctDNA. Submatrix analysis indicates at least two eigenvalues in this mixing region in both cases. The CD spectra of both Δ-[5,6] and Λ-[5,6] are virtually unchanged on addition of ctDNA. Hence the ICD spectra for these systems are negligible. The small perturbations of the CD spectra can be assigned to weak nonspecific electrostatic interactions between the DNA and ruthenium complex.[41]

The ICD spectral form for Δ-PHEN−DNA and Δ-[4,7]−DNA complexes are related, with positive maxima at 460 nm and negative maxima at 410 nm, and, for *R* greater than 1:4, a nonzero isosbestic point at 480 nm. Both Δ metal complexes show little variation in ICD spectral form with polynucleotide sequence. The spectra are similar in form to the induced normal absorption spectra and are a result of a positive change to the CD in the long-wavelength region and a negative change in the shorter wavelength region. The ratio of magnitude of the positive maxima to the negative maxima is 3:2 for the Δ-PHEN−DNA complex, whereas for the Δ-[4,7]−DNA complex, the ratio is 1:2. The ICD spectra for the Δ-[3,4,7,8]−ctDNA system takes the relative magnitude change of the 460 and 410 nm peaks even further so the positive peak is canceled by the negative maximum.

The ICD spectra for the Λ-PHEN−DNA, Λ-[4,7]−DNA, and Λ-[3,4,7,8]−DNA complexes also have a related form. ICD spectra for the Λ-PHEN and Λ-[4,7] complexes have positive maxima at 480 nm. This peak is shifted to 470 nm in the

(41) Schipper, P. E.; Rodger, A. *J. Am. Chem. Soc.* **1985**, *107*, 3459−3465

Table 2. Equilibrium Binding Constants K and Effective Binding Site Size n (i.e., the Number of DNA Bases per Metal Complex) for PHEN−DNA and [4,7]−DNA Complexes

	Δ-PHEN			Λ-PHEN		
DNA	R	n	$K/10^6$ M^{-1}	R	n	$K/10^6$ M^{-1}
ctDNA	1:15.0−37.5	12 ± 2	1.80 ± 0.50	1:10.2−37.5	8 ± 1	0.40 ± 0.05
	1:0.3−4.8	3 ± 0.1	3.00 ± 0.50	1:0.6−4.8	3 ± 1	3.50 ± 0.50
AT	1:8.3−15.7	9 ± 2	0.05 ± 0.002	1:8.3−15.7	12 ± 2	2.00 ± 1.00
	1:1.3−3.9	3 ± 0.5	0.20 ± 0.04	1:1.4−6.3	4 ±1	25.00 ± 5.00
GC	1:6.3−15.7	10 ± 0.8	1.30 ± 0.30	1:6.1−11.6	8 ± 1	0.20 ± 0.40
	1:1.4−4.2	3 ± 0.4	4.00 ± 1.00	1:1.1−4.6	*b*	*b*
	Δ-[4,7]			Λ-[4,7]		
	R	n	$K/10^6$ M^{-1}	R	n	$K/10^6$ M^{-1}
ctDNA	1:6.1−25.1	10 ± 1	4.20 ± 2.00	1:4.2−8.3	8 ± 1	0.18 ± 0.02
	1:1.1−4.1	2 ± 0.5	0.30 ± 0.10	1:0.3−2.1	2 ± 0.5	0.40 ± 0.10
AT	1:6.2−12.2	12 ± 2	2.50 ± 1.50	1:4.2−8.2	8 ± 1	0.10 ± 0.01
	1:0.4−4.5	4 ± 0.8	0.08 ± 0.06	1:0.3−2.8	3 ± 1	6.00 ± 1.00
GC	1:6.3−12.6	10 ± 1.2	5.40 ± 2.50	1:4.1−7.8	10 ± 1	1.20 ± 0.30
	1:0.5−4.4	3 ± 0.7	0.50 ± 0.10	1:0.4−2.6	3 ± 1	0.30 ± 0.05

[a] R is the mixing ratio metal complex:DNA phosphate. [b] A value was indeterminable.

Λ-[3,4,7,8]−DNA ICD spectra. All spectra display a second maximum between 410 and 385 nm. Overall, this ICD signal corresponds to a positive change in the CD in both the longer and shorter wavelength regions. The difference between the Λ-PHEN, Λ-[4,7], and Λ-[3,4,7,8] complexes is more marked when considering the variation in spectral form as mixing ratio decreases. The observed change in spectra across the titration series 1:1 to 1:30 for the DNA−Λ-PHEN complex is only slight. There is a local negative maximum at 450 nm and, for R greater than 1:4, a nonzero isosbestic point at 460 nm. In contrast, there is a distinct change in the spectra across the titration series for both the Λ-[4,7] and Λ-[3,4,7,8] complexes. There are also no negative signal and no isosbestic point in the ICD with these metal complexes. At R = 1:10 the relative magnitude of the positive maxima at 480 nm to the positive maxima at 410−380 nm is 3:2 for the Λ-PHEN−ctDNA and Λ-[4,7]−ctDNA complexes. The ratio increases to 2:1 for Λ-[3,4,7,8].

Equilibrium Binding Constants. For PHEN and [4,7], IM calculations for both enantiomers with all DNAs studied were carried out using data from regions where the form of the ICD spectra are independent of R. Plots of $([DNA]_i - [DNA]_k)/(\rho_i - \rho_k)$ versus $([DNA]_i/\rho_i - [DNA]_k/\rho_k)/(\rho_i - \rho_k)$, where $(_{i,k})$ equals all pairs of spectra in the series, were linear with slope c/ξ (c is the total metal complex concentration) and intercept ξn. The equilibrium binding association constants, K, for the equilibria

$$\text{free ligand} + \text{free binding site} \rightleftarrows \text{bound ligand}$$

and effective binding site size n (i.e., the number of phosphates or bases per bound metal complex) may then be determined. The results are shown in Table 2. The values at low R provide a lower limit for the K of the most favorable modes of binding, and the high ratio values provide an upper limit for K of the least favorable modes of binding. The error range was determined using all concentration data points. The continuous change in ICD spectroscopic form throughout the Λ-[3,4,7,8]−DNA and Δ-[3,4,7,8]−DNA titrations precludes the employment of the intrinsic method.

Computer Modeling. In a previous modeling study[4] of the PHEN−DNA complex, we focused on major groove binding and found two viable major groove binding modes for each enantiomer, in which either one chelate or two chelates are oriented toward the base pairs. These were referred to as *partially inserted* (so-called because the plane of the groove-bound single chelate is parallel with the base pair planes, but not intercalated) and *facial*. The major groove facial binding[4] was concluded to be unfavorable relative to partial insertion and is not considered further in the current work. More recent findings[6] have made us consider the possibility of minor groove binding modes. The two possible minor groove modes can have one or two chelates oriented toward the base pairs. We refer to these as *slotted* (so-called because the single chelate is aligned with the walls of the minor groove) and *minor facial*, respectively.

From the energy-minimized complexes of the partially inserted, slotted, and minor facial metal complexes we were able to determine the angle between the metal complex 3-fold axis and the DNA helical axis (α) as discussed above. The angle determined experimentally, α_{eff}, from the LD spectra is an average of all binding modes present. Hence it is possible, in principle, to determine the binding model adopted by comparing the experimental and theoretical angles. It should be emphasized that the experimental angle may in fact be a weighted average of all binding modes present that have a well-defined orientation. Thus the correct binding model orientations at a given value of R may be an average ratio of different binding modes. These results are summarized in Table 3. In some cases it was necessary to make assumptions about the relative importance of a binding mode based on the binding energies as summarized in Figure 6. The assumptions are noted in Table 3 footnotes.

Binding Model for Λ-PHEN. On the basis of only the geometrical data from the LD spectra and the computer models (Tables 1 and 3, Figure 7), it can be concluded that Λ-PHEN binds almost exclusively in the major groove in a partially inserted orientation at both low R and high R. The computed binding energies are consistent with this model as they favor partially inserted binding with most sequences (Figure 6b). The nature of the small minor groove binding component cannot be determined from the LD data, but on the basis of energy minimization a slotted orientation is more probable at all R values since the minor groove facial energies are of the order of −45 kcal/mol for Λ-PHEN (data not shown) compared with the average slotted value of approximately −52 kcal/mol (Figure 6b).

Binding Model for Δ-PHEN. The derivation of the binding model for Δ-PHEN is less straightforward than for Λ-PHEN. The experimental α_{eff} values (Tables 1 and 3) agree closely with that calculated for the partially inserted mode at low R (Table

Table 3. Experimental and Computed Angles (α_{eff}) (deg) between the DNA Helical Axis and the PHEN 3-Fold Axis[a]

metal complex	*R*	α_{eff} (exptl)	α(pi)	α(sl)	α(mifa)	% α(pi)	% α(sl)	% α(mifa)
Δ-PHEN	1:5−20	38	35[b]	84	18	*c*	32	68
	1:1	53	31	85	20	25[d]	46	29
Λ-PHEN	1:6−16	59	65	22	18	87	13	*e*
	1:1	57	68	20	20	79	21	*e*
Δ-[4,7]	1:5−20	42	53	79		*c*	41	59[f]
	1:1.5−3	54	51	77		25[g]	40	35
Λ-[4,7]	1:9−20	84	57	11		143	−43	*e*
	1:1	58	58	10		100	0	*e*

[a] The α(pi), α(sl), and α(mifa) values are the angles obtained from the energy-minimized complexes for respectively the partially inserted, slotted, and minor groove facial modes, averaged for the AT and GC complexes. The high *R* values are taken from the three metal complex complexes, and the angle was computed for the central metal complex. Some minor groove facial data is omitted as a wide range of orientations have the same energy. The final three columns give an approximate percentage occupancy of each mode subject to the assumptions given in the footnotes. [b] With AT, a single Δ-PHEN metal complex can adopt several orientations in the major groove partially inserted binding mode, and we cannot give a specific angle. With GC, an orientation with $\alpha = 35°$ was energetically favorable. [c] Assuming no pi contribution. [d] Assuming 25% pi contribution at isolated orientation. [e] Assuming no mifa contribution. [f] Assuming PHEN angles and no pi contribution. [g] Assuming 25% pi contribution at isolated orientation.

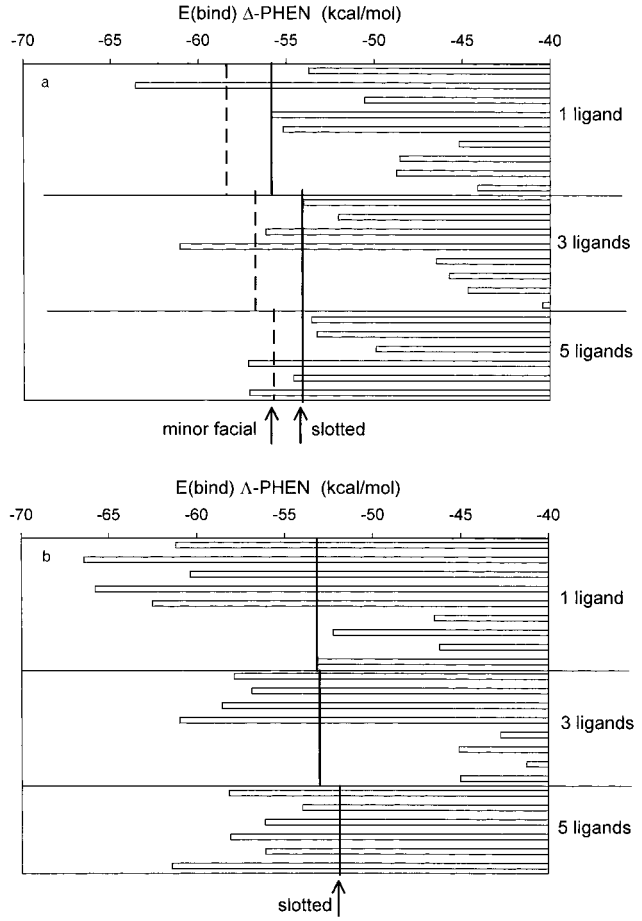

Figure 6. Summary of binding energies of the major groove partially inserted modes of (a) Δ-PHEN and (b) Λ-PHEN in low- and high-*R* regimes (i.e., 1, 3, and 5 metal complex calculations) with different sequences. The approximate energies of the minor groove modes are indicated (they are approximately sequence independent).

3) suggesting 100% partial insertion of Δ-PHEN under these conditions.[42] However, a partially inserted mode is inconsistent with the NMR data of Eriksson et al.[6] which suggested a minor groove facial binding mode. It is also inconsistent with the binding energies calculated for the partial insertion binding of Δ-PHEN compared with the slotted and minor groove facial binding modes (Figures 6a and 8). These energies suggest that both minor facial and slotted modes are more favorable than partial insertion (with the exception of 5′-GC sites). If one assumes a binding model based only on the two minor groove modes at low *R*, the experimental and computed angles suggest 30%:70% slotted:minor facial occupancy (Table 3). These percentages are consistent with the computed binding energies at low metal complex load where the minor facial is approximately 3 kcal/mol more stable than the slotted mode (Figure 6a). We note that in contrast to the situation for partially inserted binding, the minor groove binding modes do not exhibit strong sequence dependence, hence their representation in Figure 6 by an average value for all sequences.

The key feature in determining the binding mode at high *R* for Δ-PHEN is the significant change in experimental α_{eff} compared to low *R* (Tables 1 and 3). This requires a change in the occupancy ratio of the modes. On the basis of the apparent site size (typically $n = 3$ bases per metal complex) of the high-*R* binding (Table 2), and given that each metal complex occupies four bases in each mode, we conclude that both grooves are occupied. For $n = 3$, at least 25% of the bound metal complexes must be in each groove. On the basis of the calculated binding energies (Figure 6a, three and five metal complex calculations, Figure 9), the minor facial and slotted modes are generally more favorable than the partially inserted binding mode, although less so at high *R* than at low *R*. From this we conclude that the minor groove is essentially filled at high *R* and that the remaining bound metal complexes occupy the major groove in a partially inserted mode. Assuming 25% partial insertion we then deduce a binding model having 45% slotted and 30% minor facial modes (Table 3). The trend toward increasing slotted occupancy of the minor groove is also consistent with the computed binding energies under high-*R* conditions. The reduced affinity of the minor facial mode for close packed metal complexes is due to the increasing distortion of the DNA that it induces.

Binding Model for Δ-[4,7]. For Δ-[4,7] the experimental α_{eff} values are essentially the same as those for Δ-PHEN at both low and high *R* (Table 1). Given that the numbers of bases per bound metal complex for the two Δ enantiomers are also similar, we may conclude that the Δ-[4,7] binding behavior is similar to that of Δ-PHEN.

Binding Model for Λ-[4,7]. Similarly to the Δ-[4,7] metal complex, the experimental α_{eff} values for Λ-[4,7] differ for high-*R*- and low-*R*-binding conditions (Table 1). This is in contrast to the situation for Λ-PHEN where little change is apparent. The high α_{eff} value at low *R* is inconsistent with either the partially inserted or the slotted binding mode (see Λ-PHEN orientations in Table 3). We therefore conclude that, under these

(42) This is in contrast to our previous conclusions based on the A_2 assignment of the 485 nm absorption as discussed above.

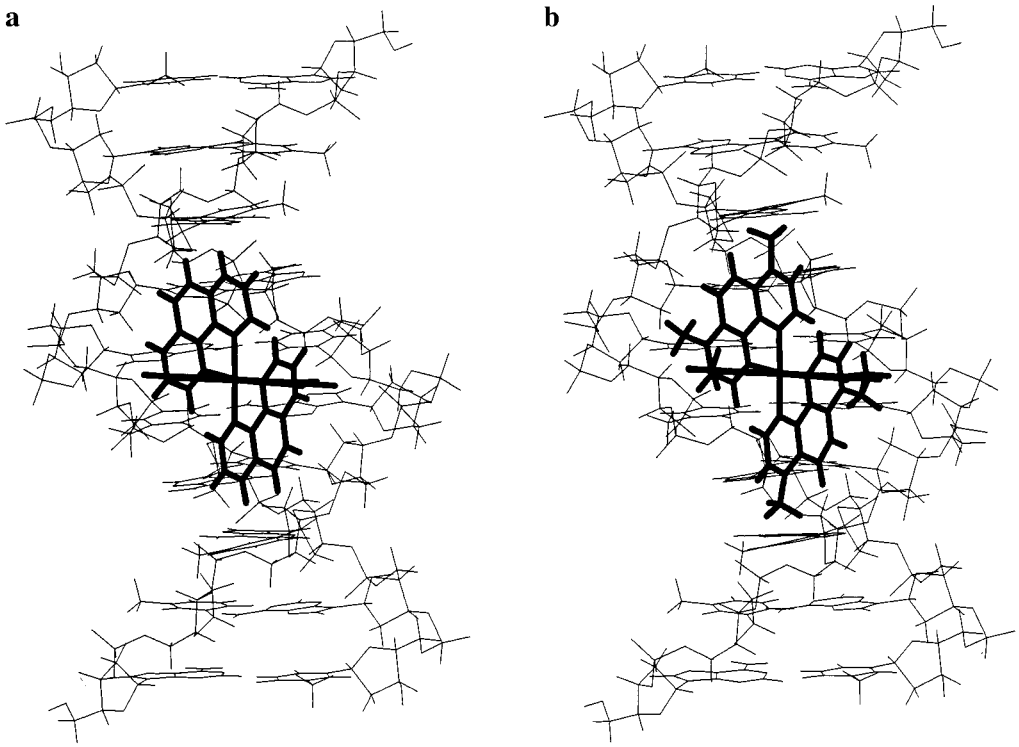

Figure 7. Partially inserted single metal complex complexes of (a) Λ-PHEN and (b) Λ-[4,7] with AT. Note the better alignment of the outer chelates of Λ-PHEN with the DNA backbone.

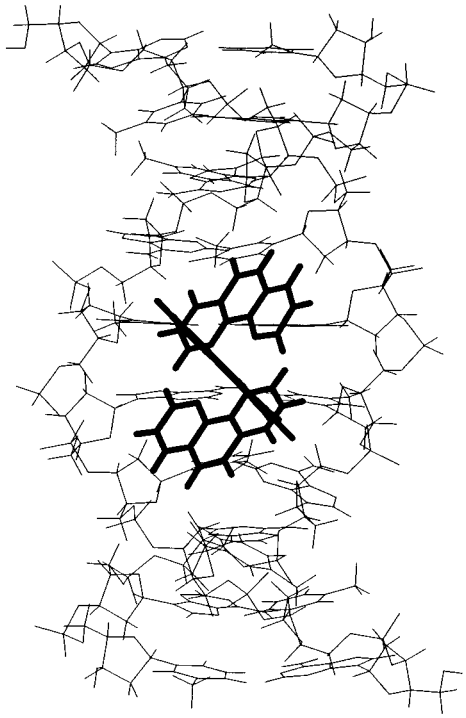

Figure 8. Minor groove facial complex of Δ-PHEN with AT, showing the expansion of the minor groove required to accommodate the complex formation.

conditions, the binding of Λ-[4,7] is dominated by a minor groove facial mode oriented with a large angle (close to 90°) between the DNA helix axis and the metal complex 3-fold axis. Consistent with the argument made for Δ-PHEN and Δ-[4,7], it is likely that close packing of such a minor groove facial mode (high *R*) is unfavorable due to DNA distortion and a second mode becomes increasingly occupied as the metal complex density increases (Figure 7).

Conclusion

The combination of dichroism data and computer modeling has proved effective in elucidating the PHEN/DNA and [4,7]/DNA interactions. The data favor a model that at low metal complex:DNA base ratio has Λ-PHEN in the partially inserted orientation in the major groove while Δ-PHEN favors a minor groove facial site. A model having only a single preferred binding mode for each enantiomer is consistent with previous work as discussed above. The minor facial binding mode proposed for Δ-PHEN is very similar to that deduced from NMR NOESY experiments.[6] Although a small percentage (15% and 30%, respectively) of a second mode is proposed for each enantiomer, it is likely that most experimental techniques are unable to directly observe this mode. This has been previously suggested in the context of fluorescence lifetime experiments.[5] It may also be that certain experimental approaches are able to detect one mode more easily than another. This may account for the observation only of a slotted minor groove mode for Λ-PHEN in NOESY experiments.[6] In this experiment the long mixing times (200 and 450 ms) required to see the slotted mode make it unsurprising that the technique missed a major groove mode where greater metal complex mobility is expected as the DNA breathes. In the current work we cannot accommodate a large percentage of slotted mode for Λ-PHEN at low *R* as the experimental α_{eff} angle is too large compared to the slotted orientation (Table 3).

For Δ-PHEN at low *R*, insertion of two chelates into the minor groove can be achieved as shown by Eriksson et al.[6] but only with significant distortion of the DNA. This distortion may be responsible for the reduced orientation of the DNA duplex observed at low concentration of the Δ enantiomer, an effect that has not previously been satisfactorily accounted for.[7] The increased distortion of DNA that would be caused by close packing of minor facial metal complexes explains the diminished percentage occupancy of the minor facial occupancy for Δ-PHEN at high *R* (Table 3). This is again consistent with the

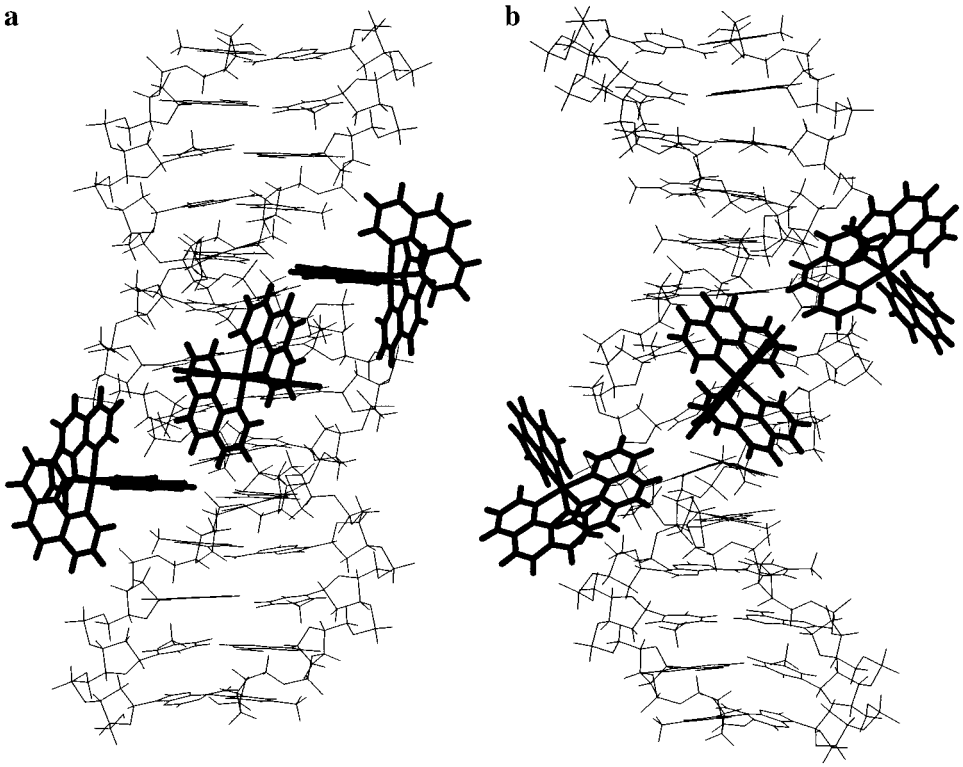

Figure 9. Potential close packed complexes of Δ-PHEN with AT having (a) partially inserted and (b) slotted metal complexes. In part b the DNA deformation is significant, making this complex unfavorable.

initial loss of DNA orientation observed by Hiort et al. at low metal complex load[7] and the subsequent (at $R = 1{:}50$) maintenance of the orientation with addition of metal complexes. It is of note that no such reduction of orientation occurs for Λ. The slight increase in orientation with addition of Λ-PHEN[7] is consistent with a mode that is "pseudointercalative", i.e., partial insertion, because such a mode would be expected to stiffen the DNA helix.

Haq et al.[43] have shown that the enthalpy of binding of PHEN to DNA is +2.5 kcal/mol (10.5 kJ mol^{-1}), which, given an average equilibrium constant of 10^6 mol^{-1}, gives an entropy change on binding of approximately 150 J mol^{-1} K^{-1}. This large entropic contribution implies that the binding is entropically driven by the metal complex displacing water molecules from the DNA grooves upon binding. However, our energy arguments have been very successful in accounting for the trends in the binding behavior as a function of metal complex enantiomer and DNA sequence. Thus one can assume that there is no significant difference in the entropy contributions for the three binding modes, and the differences in their behavior are enthalpically determined.

With the Δ-[4,7]−DNA complexes the methyl substituents increase the stability of the binding at low *R* compared to Δ-PHEN. This may be a result of the increased entropic effect caused by the location of two dimethylated chelates in the minor groove in a facial mode. For Λ at low *R*, the methyl substituents on average do not increase the stability of the binding. This is probably the result of a competition between the stabilizing entropic effect and the necessity for adopting the less favorable minor facial binding mode due to the steric requirements of the methyl groups in the partially inserted mode. At high *R*, the Λ-[4,7] and Δ-[4,7] equilibrium binding constants decrease with respect to those of the corresponding PHEN complexes by an order of magnitude. This may be a result of the loss of strong binding in any of the three orientations. The minor facial mode is not favorable under close packed conditions due to the excessive DNA distortion, and the partially inserted mode is also unfavorable because of the methyl steric clashes. The slotted mode may be sterically acceptable, but it has the hydrophobic disadvantage of exposing four methyl groups in the outer chelates to the solvent.

The [3,4,7,8] complexes may be concluded to be increasing the trend toward minor groove facial binding at low *R* with an even greater increase in DNA distortion resulting in no orientation of the metal complex observable in the LD experiment and the high-*R* aggregation of the DNA.

As there is no evidence of the [5,6] metal complexes binding to DNA, it is reasonable to conclude that the methyl groups in the center of the chelate ensure that the minor groove and partial insertion modes are sterically unfavorable.

Acknowledgment. The authors are grateful to Dr. Graham Richards and Dr. Adrian Elcock for their discussion of the work in the manuscript. We acknowledge support of the NIH (I.S.H., CA64299-01 and PO1-HL60231) and NATO (Grant: CRG-970290).

IC990654C

(43) Haq, I.; Lincoln, P.; Suh, D. C.; Nordén, B.; Chowdhry, B. Z.; Chaires, J. B. *J. Am. Chem. Soc.* **1995**, *117*, 4788−4796.